



This is a repository copy of *Modelling and Identification of a Three-Phase Eclectric Arc Furnace*.

White Rose Research Online URL for this paper:
<http://eprints.whiterose.ac.uk/75818/>

Monograph:

Billings, S.A. (1979) *Modelling and Identification of a Three-Phase Eclectric Arc Furnace*. Research Report. ACSE Report 87 . Department of Control Engineering, University of Sheffield, Mappin Street, Sheffield

Reuse

Unless indicated otherwise, fulltext items are protected by copyright with all rights reserved. The copyright exception in section 29 of the Copyright, Designs and Patents Act 1988 allows the making of a single copy solely for the purpose of non-commercial research or private study within the limits of fair dealing. The publisher or other rights-holder may allow further reproduction and re-use of this version - refer to the White Rose Research Online record for this item. Where records identify the publisher as the copyright holder, users can verify any specific terms of use on the publisher's website.

Takedown

If you consider content in White Rose Research Online to be in breach of UK law, please notify us by emailing eprints@whiterose.ac.uk including the URL of the record and the reason for the withdrawal request.



eprints@whiterose.ac.uk
<https://eprints.whiterose.ac.uk/>

MODELLING AND IDENTIFICATION OF
A THREE-PHASE ELECTRIC ARC FURNACE

by

S. A. Billings, B.Eng., Ph.D., M.Inst.M.C., AMIEE

Department of Control Engineering
University of Sheffield
Mappin Street
Sheffield S1 3JD

Research Report No. 87

May 1979

Introduction

This chapter is an attempt to illustrate the development of a mathematical model of an industrial process by combining analytical modelling techniques with a system identification study. Although both these approaches can often be applied in isolation to develop a mathematical description of a process the lack of detailed knowledge of the high power arc discharge suggests a combination of these techniques in the case of the electric arc furnace.

The objective of the present study is to develop three-phase models of both arc impedance and arc current controlled electric arc furnaces. Initially a single-phase model of the electrode position controller, arc discharge and furnace transmission system are developed for an arc impedance controlled furnace using analytical modelling techniques and assuming zero interaction between the three regulators. The assumptions and approximations associated with this model are investigated by designing experiments and conducting tests on a production arc furnace. Properties of the arc discharge, interaction between the regulators and a pulse transfer function representation of the electrode position controller are identified. These results are extended and three-phase models of an arc impedance and arc current controlled electric arc furnace are derived.

The electric arc furnace

Electric arc furnaces are widely used throughout the world to melt and refine steel. The present study relates to a 135 tonne 35MVA production arc furnace. The furnace consists of a refractory lined shell with three electrodes which pass through holes in the roof. The roof and electrode structure can be swung aside in a horizontal plane to permit scrap charging from an overhead basket. Electrical power is supplied to the furnace electrodes through bus-bars and water cooled flexible cables from the furnace transformer. Heat is transferred to the scrap steel from electric arcs (typically 36kA at 560v) drawn between the tips of the electrodes and the metallic charge. A schematic diagram of the arc impedance controlled furnace is illustrated in Fig. 1.

Throughout the period of a melt the arc length varies erratically due to scrap movement within the furnace and some form of control is required to maintain the desired power input level. The existing control philosophy is based upon both short and long term control policies. The long term policy consists of manually adjusting the power input to the furnace at various stages of the melt by selection of a suitable transformer voltage tap. Short term dynamic control is based upon maintaining a preselected constant arc impedance by adjusting the electrode position in response to disturbances. Each electrode is individually positioned by an electrode position controller which attempts to maintain a reference arc impedance compatible with the long term power input schedule.

Single-phase model

Although a considerable amount of research has been directed towards improving the melting efficiency of the electric arc furnace there are many aspects of its operation and control which require further study. Various authors^{1,2,3} have developed single-phase models of electric arc furnace control systems but very little work has been directed towards studying the properties of the high power arc discharge^{4,5} and its effects upon short term dynamic control.

The servomechanism for positioning the electrodes in the furnace under investigation is typical of many installations and consists of an amplidyne Ward-Leonard regulator operating on an arc impedance error signal. A circuit diagram of one of the three electrode position controllers is illustrated in Fig. 2.

The arc impedance measuring circuit compares currents proportional to transformer secondary voltage and arc current and produces an error signal when they are unequal. Under steady-state conditions the error signal ϵ can be represented by

$$\epsilon = G_5 I_1 - G_4 V_{ml} \quad (1)$$

hence the term arc impedance control. The error signal is applied to the control winding and excites the amplidyne Ward-Leonard drive which positions the electrode through suitable gearing and a winch system.

Interaction between the three electrode regulators is minimised when operating under arc impedance control. The interaction which arises from properties of the arc discharge may not however be

negligible although all previous work has assumed this to be the case. Properties of the arc discharge will be investigated in later sections but a single-phase model will be derived initially to provide insight and aid the design of experiments on the furnace.

The Ward-Leonard drive can be modelled using transfer function relationships, derived by analysing equivalent circuits of the electrical machines and can be represented as shown in Fig. 3. The defining state-space equations can then be determined as follows⁶, using the symbols defined in Fig. 3

$$\text{amplidyne: } \dot{x}_1 = \{(-DG_4 - AG_5)x_9 - F_D x_3 - F_S x_2 - x_1\} / T_1 \quad (2)$$

$$\dot{x}_2 = (k_1 x_1 - x_2) / T_2 \quad (3)$$

$$\text{generator: } \dot{x}_3 = (K_2 x_2 - K_2 K_E x_4 - x_3) / T_3 \quad (4)$$

$$\text{motor: } \dot{x}_4 = (x_3 - F_B x_6 - x_4) / T_4 \quad (5)$$

$$\dot{x}_5 = (G_1 x_4 - x_5) / T_5 \quad (6)$$

$$\dot{x}_6 = x_5 / G_2 \quad (7)$$

$$\dot{x}_7 = G_3 x_6 \quad (8)$$

$$\text{mast dynamics: } \dot{x}_8 = \omega_N^2 (x_7 - x_9) - 2\zeta\omega_N x_8 \quad (9)$$

$$\dot{x}_9 = x_8 \quad (10)$$

The weight of the electrodes and supporting mast structure is pneumatically counterbalanced and the dynamics of the electrode are represented in the model by a damped second order system. Values of the natural frequency and damping coefficient have been estimated from plant trials using accelerometers connected to the electrode tip.

The single-phase furnace transmission system interconnecting the supply and arc furnace, illustrated in Fig. 4, can be represented by^{2,6}

$$I_1 = E(\alpha Z_{t2} - Z_{t3}) \left(\sum_{i,\ell=1}^3 Z_{ti} Z_{t\ell} \right) i \neq \ell \quad (11)$$

$$Z_{ti} = (R_{ai} + R_{ci}) + jX_i = R_{ti} + jX_i \quad (12)$$

where Z_{ti} are the total phase impedances referred to the transformer secondary and R_{ai} represent arc resistances, R_{ci} the system line resistances, X_i the line reactances, E the line voltage and α the complex 3-phase operator. The current magnitude may then be obtained in the form

$$I_1^2 = \frac{E^2 \{ (-R_{t3} - R_{t2}/2 - \sqrt{3}X_2/2)^2 + (\sqrt{3}R_{t2}/2 - X_2/2 - X_3)^2 \}}{\left\{ \sum_{i,\ell=1}^3 (R_{ti}R_{t\ell} - X_iX_\ell) \right\}^2 + \left\{ \sum_{i,\ell=1}^3 R_{ti}X_\ell \right\}^2} \quad i \neq \ell \quad (13)$$

Linearizing by taking a first order Taylor series expansion of eqn (13) with $I_1 = I_1^0 + i_1$, $R_{ai} = R_{ai}^0 + r_{ai}$ and assuming no interaction between the arc impedances gives the arc current/arc resistance relationship

$$i_1/r_{ai} = \frac{(-I_1^0)^3 \left\{ (R_{t2} + R_{t3}) \sum_{i,\ell=1}^3 (R_{ti}R_{t\ell} - X_iX_\ell) + (X_3 + X_2) \sum_{i,\ell=1}^3 R_{ti}X_\ell \right\}}{E^2 \{ (-R_{t3} - R_{t2}/2 - \sqrt{3}X_2/2)^2 + (\sqrt{3}R_{t2}/2 - X_2/2 - X_3)^2 \}} \quad i \neq \ell$$

or $i_1/r_{ai} = -F_1 \quad (14)$

The arc discharge model relating arc voltage V_a and arc length H is based on Nottingham's empirical equation⁷ which is an approximation to the static dc arc characteristic for similar

electrode materials

$$V_{a1} = A_1 + D_1 H_1 + \frac{C_1 + B_1 H_1}{I_1^n} \quad (15)$$

In the electric arc furnace the discharge is an ac arc and the electrodes are graphite and steel, obviously dissimilar materials. However, the inherent nonlinearities of the high current ac arc make its mathematical representation vary difficult and experimental work on arcs of this power is almost nonexistent⁵.

For long high power arcs eqn (15) can be approximated by the steady-state solution of Cassie's equation

$$V_{a1} = A_1 + D_1 H_1 \quad (16)$$

where D_1 is the arc discharge coefficient. The voltage signals V_m which provide a component of the error current in the amplidyne control field are measured at the transformer secondary terminals as indicated in Fig. 4. The voltage at this point is the resultant of the voltage across the distributed impedances in the supply cables and the resistance of the arc, and does not represent arc voltage. Arc voltage given by eqn (16) exists across the tip of the electrode and the scrap steel, and is almost impossible to measure on a production arc furnace. Consequently, the measured voltage magnitude may be expressed in the form⁶

$$V_{m1} = I_1 \{(R_{a1} + R_{c1})^2 + X_1^2\}^{\frac{1}{2}} = \{(A_1 + D_1 H_1 + I_1 R_{c1})^2 + I_1^2 X_1^2\}^{\frac{1}{2}} \quad (17)$$

where I_1 represents arc current as a reference vector. Linearizing eqn (17) using a first order Taylor series expansion and defining

$$|Z_{t1}| = \{(R_{al} + R_{cl})^2 + X_1^2\}^{\frac{1}{2}}, I_1 = I_1^o + i_1 \text{ and } R_{al} = R_{al}^o + r_{al}$$

gives

$$\begin{aligned} v_{m1} &= i_1 |Z_{t1}| + r_{al} I_1^o (R_{al}^o + R_{cl}) |Z_{t1}|^{-1} \\ &= \{(D_1 h_1 + i_1 R_{cl}) (R_{al}^o + R_{cl}) + i_1 X_1^2\} |Z_{t1}|^{-1} \end{aligned} \quad (18)$$

Including the relationship $i_1/r_{al} = -F_1$ derived from the analysis of the transmission system gives the change in arc current as

$$i_1 = \frac{F_1 D_1 h_1}{F_1 R_{al}^o - I_1^o} \text{ or } i_1 = -W_1 D_1 h_1 = -A_1 h_1 \quad (19)$$

where the constant A_1 is usually called arc gain. Substituting equation (19) into eqn (18) gives the relationship between changes in the measured voltage v_{m1} and arc length h_1

$$\begin{aligned} v_{m1} &= D_1 h_1 \{(1 - W_1 R_{cl}) (R_{al}^o + R_{cl}) - W X_1^2\} |Z_{t1}|^{-1} \\ \text{or } v_{m1} &= D_1' h_1 \end{aligned} \quad (20)$$

where D_1' is defined as the discharge coefficient^{6,7}. Eliminating v_{m1} and i_1 from eqn (18) and rearranging gives the arc resistance/arc length relationship^{6,7}

$$\begin{aligned} r_{al} &= \frac{h_1 (D_1' + (WD)_1 |Z_{t1}|)}{I_1^o R_{t1} |Z_{t1}|^{-1}} \\ \text{or } r_{al} &= B_1 h_1 \end{aligned} \quad (21)$$

Equations (19) and (20) define the relationship between the change in arc length and the change in the current and voltage signals

feedback to the arc impedance measuring circuit

$$\varepsilon_1 = -\{G_5 A_1 + G_4 D_1'\} h_1 \quad (22)$$

Small changes in the arc length have to be considered because only changes in electrode position can be conveniently measured on a production furnace.

Combining the models of the electrode position controller, arc discharge and transmission system provides a complete mathematical description of a single phase of the furnace control system as illustrated in Fig. 3. However the derivation of this model involved making numerous assumptions which cannot be verified analytically. It was assumed that Nottingham's equation provides an adequate representation of the arc and that the interaction between the three regulators is negligible. Both these assumptions must be investigated before an improved control system can be designed using the derived model. This can best be achieved by conducting experiments on the furnace and identifying the properties of interest⁹.

Identification of the furnace control system

The arc discharge

The basic aims of the identification were threefold and included, identification of properties of arc discharge, investigation of the interaction between the regulators of an arc impedance controlled furnace and identification of a model of the Ward-Leonard drive or electrode position controller.

The diversity of the identification requirements entailed designing several experiments and recording a large amount of data. This was usually done in an iterative manner so that initial experiments added to the knowledge of the process and suggested the form of future experiments. In all the experiments the data was recorded on an analogue tape recorder prior to sampling and subsequent digital analysis^{6,9,10}.

Initially, normal operating data for a typical melt was recorded to enable the relationship between electrode position, transformer secondary voltage and arc current to be investigated. A typical sequence of normal operating data is illustrated in Fig. 5.

The normal operating data was analysed to determine the discharge coefficient eqn (20) and the arc gain eqn (19). During the first basket, at the beginning of the melt, the discharge coefficient D' was found typically to be 3764V/m with an arc gain A of 859kA/m. The values of the discharge coefficient (1653V/m) and arc gain (367kA/m) estimated during refining were notably lower than those experienced during the first basket.

Dynamic volt-ampere characteristics of the arc discharge in a production furnace during refining and at the beginning of the melt are illustrated in Fig. 6. The instability of the characteristics at the beginning of the melt indicates the dependence of the arc characteristics on the furnace environment^{6,8,9,10}.

These results tend to suggest that Nottingham's equation can only be used to represent the arc discharge when D_1' and A_1 are functions of furnace environment. This can be substantiated by combining the experimental results with a simple analysis of the model^{8,9}.

Consider the effects of a step disturbance in the arc length over the period of a melt. When the furnace is cold, at the beginning of the melt, a step change in the arc length of amplitude h' will be sufficient to cause a current change i , thus

$$i = -A_{\text{cold}} h' \quad (23)$$

Towards the end of the melt, when the furnace is hot and the atmosphere ionized, a step change in arc length of amplitude h'' will be required to cause a similar change in arc current

$$i = -A_{\text{hot}} h'' \quad (24)$$

where $h'' > h'$, and hence $A_{\text{cold}} > A_{\text{hot}}$. Since the discharge coefficient D' is a function of the arc gain A and the resistance and reactance of the secondary conductors

$$D_1' = \frac{\{(1 - W_1 R_{cl}) (R_{al}^o + R_{cl}) - W_1 X_1^2\} A_1}{W_1 |Z_{t1}|}$$

$$\text{or } D_1' = A_1 Q_1 \quad (25)$$

the relationship between the arc-impedance error function and the change in arc length eqn (1) can be expressed as

$$\epsilon_1 = -(G_5 + G_4 Q_1) A_1 h_1 \quad (26)$$

Hence ϵ_1 the error feedback signal will vary considerably over the period of a melt. This will inevitably affect the overall loop gain and sensitivity of the electrode regulator and explains why the performance varies between the two extremes of unstable and highly overdamped responses^{8,9}.

A review of the literature on low current arcs reveals that the electrical conductivity of the arc is heavily dependent upon arc temperature¹¹. Moreover, at sufficiently high arc currents the localised ambient temperature can be shown to affect the temperature of the arc plasma which in turn will affect the relationship between arc impedance and arc length⁸. It would therefore appear that eqns (19) and (20) can only be used to represent high power a.c. arcs when D_1' and A_1 are functions of ambient arc temperature.

Interaction between the regulators

Interaction between the three electrode regulators is minimised when operating under arc impedance control. If the arc discharge had the properties of a metallic conductor when a disturbance occurred on one phase all the currents and voltages would change but only the impedance of the disturbed phase would be altered. However the resistance of low power arcs of a given length depend on the arc current¹¹, and if the current changes considerably the impedance may be affected. Unfortunately, no results are available for high power ac arcs and hence these properties must be investigated experimentally^{6,8,9,10}.

Because there is no interaction between the three Ward-Leonard drives any interaction between the electrode regulators must be a combination of the mutual coupling of the high current carrying conductors, which can be shown to be less than 10%⁹, and the dependence of arc impedance upon arc current. Identification of the interaction between the electrode regulators is therefore a

simple means of investigating the relationship between arc impedance and arc current for high power ac arcs.

A schematic diagram of the three-phase system is illustrated in Fig. 7. A 127 bit 33.3ms PRBS sequence was injected into the control winding of phase 2 electrode position controller, with the furnace in normal operation during refining. An on-line correlator was then used to identify the impulse responses relating the input on phase 2 to the three electrode positions. If there is any interaction between the regulators the cross-correlations will be representative of the impulse response of the interacting system. Inspection of the correlation functions, Fig. 8, confirms that there is minimal interaction when operating under arc impedance control.

However, the PRBS input may have been of insufficient power to excite the interacting modes of the system or overcome any deadzone or stiction associated with the regulators. Thus as a further check on the interaction, manual step disturbances were applied to the electrode position controller with the furnace in normal steady-state production during refining. The disturbances were applied by manually raising each electrode in turn and allowing the controller to re-establish the preset arc impedance with the other electrodes under normal automatic control. All the results indicated that the interaction is less than 10% confirming the correlation analysis.

The lack of interaction between the electrode regulators implies that arc impedance is practically independent of arc current. The regulators operating under arc impedance control can therefore be considered as three independent electrode position controllers^{6,12}.

Identification of the electrode position controller

Having established that the three regulators can be considered as independent it is only necessary to identify a model of a single phase electrode position controller. This was achieved by performing open-loop tests on the furnace with the arc discharge extinguished^{6,10}.

Initially, step inputs were applied to the open loop system to check the linearity of the system over the operating range, estimate the system gain and assess the characteristics of the noise. Various PRBS sequences were then injected into the amplidyne control field and motor speed and electrode movement recorded. The signals were digitized and analysed using an interactive identification package¹⁰. Many techniques including generalized least squares parameter estimation, step and correlation analysis were applied to extract the maximum information from the data in an efficient manner, and a difference equation model was estimated

$$g_{kk}(z^{-1}) = \frac{z^{-2T}(0.249z^{-1} + 0.3079z^{-2} + 0.095z^{-3}) \cdot 10^{-3}}{1 - 3.547z^{-1} + 4.826z^{-2} - 2.9967z^{-3} + 0.7177z^{-4}} \quad (27)$$

$$k = 1, 2, 3, T = 1/24 \text{ secs}$$

Various model order and validity checks were applied to ensure that the model provided an adequate representation of the electrode position controller.

Thus combining the identification results of the arc discharge, interaction between the regulators, and the electrode position controller provides a complete description of the furnace control system.

All the assumptions necessary in the derivation of the analytical model and the formulation of the identification results have been rigorously investigated on a production furnace. The analytical and identified models have been shown to have almost identical responses and the latter model can now be generalised to the three-phase case.

Three-phase models

Although arc impedance control is widely adopted in arc furnace regulation occasionally arc current control is implemented. Three-phase models of arc impedance and arc current controlled regulators can now be derived based on the identification results for the electrode position controller, arc discharge and interaction between the phases^{12,13}.

Three-phase impedance controlled model

The furnace transmission system illustrated in Fig. 4 can be represented by

$$I_1 = E(\alpha Z_{t2} - Z_{t3}) / \left(\sum_{k, \ell=1}^3 Z_{tk} Z_{t\ell} \right) \quad (28)$$

$$I_2 = E(Z_{t3} - \alpha^2 Z_{t1}) / \left(\sum_{k, \ell=1}^3 Z_{tk} Z_{t\ell} \right) \quad (29)$$

$$I_3 = E(\alpha^2 Z_{t1} - \alpha Z_{t2}) / \left(\sum_{k, \ell=1}^3 Z_{tk} Z_{t\ell} \right) \quad (30)$$

$$k \neq \ell$$

where the impedances are defined by eqn (12). The current magnitudes

can then be evaluated as

$$I_1^2 = E^2 [(-R_{t3} - R_{t2}/2 - \sqrt{3}X_2/2)^2 + (\sqrt{3}R_{t2}/2 - X_2/2 - X_3)^2] / Z_e \quad (31)$$

$$I_2^2 = E^2 [(R_{t3} + R_{t1}/2 - \sqrt{3}X_1/2)^2 + (X_3 + X_1/2 + \sqrt{3}R_{t1}/2)^2] / Z_e \quad (32)$$

$$I_3^2 = E^2 [(-R_{t1} + \sqrt{3}X_1 + R_{t2} + \sqrt{3}X_2)^2 + (-X_1 - \sqrt{3}R_{t1} + X_2 - \sqrt{3}R_{t2})^2] / Z_e \quad (33)$$

where

$$Z_e = \left(\sum_{k,\ell=1}^3 (R_{tk} R_{t\ell} - X_k X_\ell) \right)^2 + \left(\sum_{k,\ell=1}^3 R_{tk} X_\ell \right)^2 \quad (34)$$

and $k \neq \ell$.

Linearising using a first order Taylor series expansion with $I_k = I_k^o + i_k$, $k = 1, 2, 3$ and $R_{ai} = R_{ai}^o + r_{ai}$ in eqn's (31), (32) and (33) for $i = 1$, $i = 2$, $i = 3$ respectively, and assuming zero interaction between the three arc resistances and an infinitely stiff supply voltage yields, analogous to eqn (14),

$$i_k = -F_k r_{ak} \quad , \quad k = 1, 2, 3 \quad (35)$$

Similarly extending the derivation of the arc model in eqn's (15) to (21) to three phases and assuming zero interaction yields

$$\epsilon_k = -\{G_{5k} A_k + G_{4k} D'_k\} h_k \quad , \quad k = 1, 2, 3 \quad (36)$$

which combined with the identified model of the electrode position controller

$$h_k = g_{kk}(z^{-1}) \epsilon_k \quad , \quad k = 1, 2, 3 \quad (37)$$

where $g_{kk}(z^{-1})$ is given by eqn (27), defines the three-phase arc impedance controlled furnace model^{12,13}.

Three phase current controlled model

In a three phase arc furnace operating under current control the electrode position controllers attempt to maintain the arc current at their reference values. If a disturbance occurs all the arc currents will change and the three electrode regulators operate to re-establish the desired power input level. The regulation is therefore spread over all three electrode regulators which are no longer non-interacting.

Although it is assumed that there is no inherent interaction between the arc impedances, the operation of all the regulators to clear a disturbance suggests that the arc currents can be represented by a relationship of the form

$$i_k = f_k (r_{a1}, r_{a2}, r_{a3}) \quad k = 1, 2, 3 \quad (38)$$

Such a relationship can be obtained by linearizing the current magnitude, eqn's (31), (32) and (33) using a first order Taylor series expansion with $I_k = I_k^0 + i_k$, $R_{ak} = R_{ak}^0 + r_{ak}$, $k = 1, 2, 3$ to yield

$$i_1 = E^2 [\alpha_1 r_{a1} + \beta_1 r_{a2} + \gamma_1 r_{a3}] / I_1^0 Z_e^2 \quad (39)$$

$$i_2 = E^2 [\alpha_2 r_{a1} + \beta_2 r_{a2} + \gamma_2 r_{a3}] / I_2^0 Z_e^2 \quad (40)$$

$$i_3 = E^2 [\alpha_3 r_{a1} + \beta_3 r_{a2} + \gamma_3 r_{a3}] / I_3^0 Z_e^2 \quad (41)$$

$k \neq l$, relating the change in the arc currents to the changes in the arc resistances as the latter are adjusted by the electrode regulators. Eliminating r_{a1} , r_{a2} and r_{a3} using eqn (21) gives the current controlled transmission system model

$$\begin{pmatrix} i_1 \\ i_2 \\ i_3 \end{pmatrix} = E^2/Z_e^2 \begin{pmatrix} \frac{B_1\alpha_1}{I_1^o} & \frac{B_2\beta_1}{I_1^o} & \frac{B_3\gamma_1}{I_1^o} \\ \frac{B_1\alpha_2}{I_2^o} & \frac{B_2\beta_2}{I_2^o} & \frac{B_3\gamma_2}{I_2^o} \\ \frac{B_1\alpha_3}{I_3^o} & \frac{B_2\beta_3}{I_3^o} & \frac{B_3\gamma_3}{I_3^o} \end{pmatrix} \begin{pmatrix} h_1 \\ h_2 \\ h_3 \end{pmatrix} \quad (42)$$

with $k \neq l$ where α_k , β_k and γ_k are constants which depend upon the arc characteristics and the impedance of the secondary conductors.

Combining eqn (37) with eqn (42) and the current controlled model for the error feedback to the amplidyne

$$\epsilon_k = -N_k i_k \quad , \quad k = 1,2,3 \quad (43)$$

where N_k is a constant feedback gain, defines the interacting three-phase current controlled furnace model^{9,12} illustrated in Fig. 9.

Note that the arc characteristics D_k' , A_k and B_k in the three-phase models depend upon the ambient arc temperature and can therefore take a range of values as identified in previous sections. This also implies that the interaction between the regulators of a current controlled furnace eqn (42) will depend upon the characteristics of the arc of each phase. Localised changes in the arc environment, which may be caused by vapourisation of impurities in the steel, will therefore affect the degree of interaction between the phases.

The current and impedance controlled models have been formulated assuming equal arc characteristics and electrode position controller

dynamics. Such conditions often prevail in arc furnace operation. However, the models are not restrictive and can be used to simulate the effects of unequal arc characteristics or electrode position controller dynamics if required.

Conclusions

Three-phase models of an arc impedance and an arc current controlled electric arc furnace have been derived by combining analytically derived models with the results of an identification study. Although the simplifying assumptions which are often necessary in the derivation of an analytical model can usually be made with confidence based on the available literature and experience of modelling similar processes this approach was precluded in the case of the electric arc furnace because of the lack of detailed knowledge of the high power arc discharge. However, by deriving a simple single phase model to gain insight into the process operation, experiments were designed and the modelling assumptions were investigated using identification techniques. It was shown that properties of the electric arc discharge are heavily dependent upon ambient arc temperature and that arc impedance is virtually independent of arc current in arcs of this power. By incorporating this information in the single phase model and extending this to a three-phase representation using the identified model of the electrode position controller an accurate mathematical description of an arc impedance and arc current controlled furnace was derived.

The three-phase models have been successfully used to design improved control schemes for the arc furnace¹³ including a dual impedance/current control strategy¹², a temperature weighting adaptive controller⁸ and p.i.d. and minimum variance regulators⁹.

References

1. Brown, P., Langman, R.D.: Simulation of closed loop energy control applied to arc furnaces; Journal Iron and Steel Inst., Aug 1967, pp.837-847.
2. Nicholson, H., Roebuck, R.: Simulation and control of electrode position controllers for electric arc furnaces; Automatica, 8, 1972, pp.683-693.
3. Morris, A.S., Sterling, M.J.H.: Analysis of electrode position controllers for electric arc steelmaking furnaces; Iron and Steel International, 48, Aug 1975, pp.291-298.
4. Bowman, B., Jordan, G.R., Fitzgerald, F.: The physics of high current arcs; Journal of the Iron and Steel Inst., 1969, pp.798-805.
5. Bowman, B., Jordan, G.R., Wakelam, D.: Electrical and photographic measurements of high power arcs; J. Phys. D. Appl. Phys., 3, 1970, pp.1089-1099.
6. Billings, S.A., Nicholson, H.: Identification of an electric arc furnace electrode control system; Proc.IEE, 122, 1975, pp.849-856.
7. Browne, T.E. (Jnr): The electric arc as a circuit element; Journal of the Electrochemical Soc., Jan 1955, pp.27-37.

8. Billings, S.A., Nicholson, H.: Temperature weighting adaptive controller for electric arc furnaces; *Ironmaking and Steelmaking*, 4, 1977, pp.216-221.
9. Billings, S.A.: Modelling, identification and control of an electric arc furnace; Ph.D. thesis, Sheffield Univ., 1975.
10. Billings, S.A., Sterling, M.J.H., Batey, D.J.: SPAID - an interactive data analysis package and its application to the identification of an electric arc furnace control system; IEE Conf. Publ. 159, Random Signals Analysis, April 1977, pp.161-170.
11. S. C. Haydon (Editor): Discharge and plasma physics; Armidale, NSW, Univ. of New England, 1964.
12. Billings, S.A., Nicholson, H.: Modelling a three-phase electric arc furnace; a comparative study of control strategies; *Applied Mathematical Modelling*, 1, 1977, pp.355-361.
13. Billings, S.A., Boland, F.M., Nicholson, H.: Electric arc furnace modelling and control; *Automatica*, 15, 1979, pp.137-149.

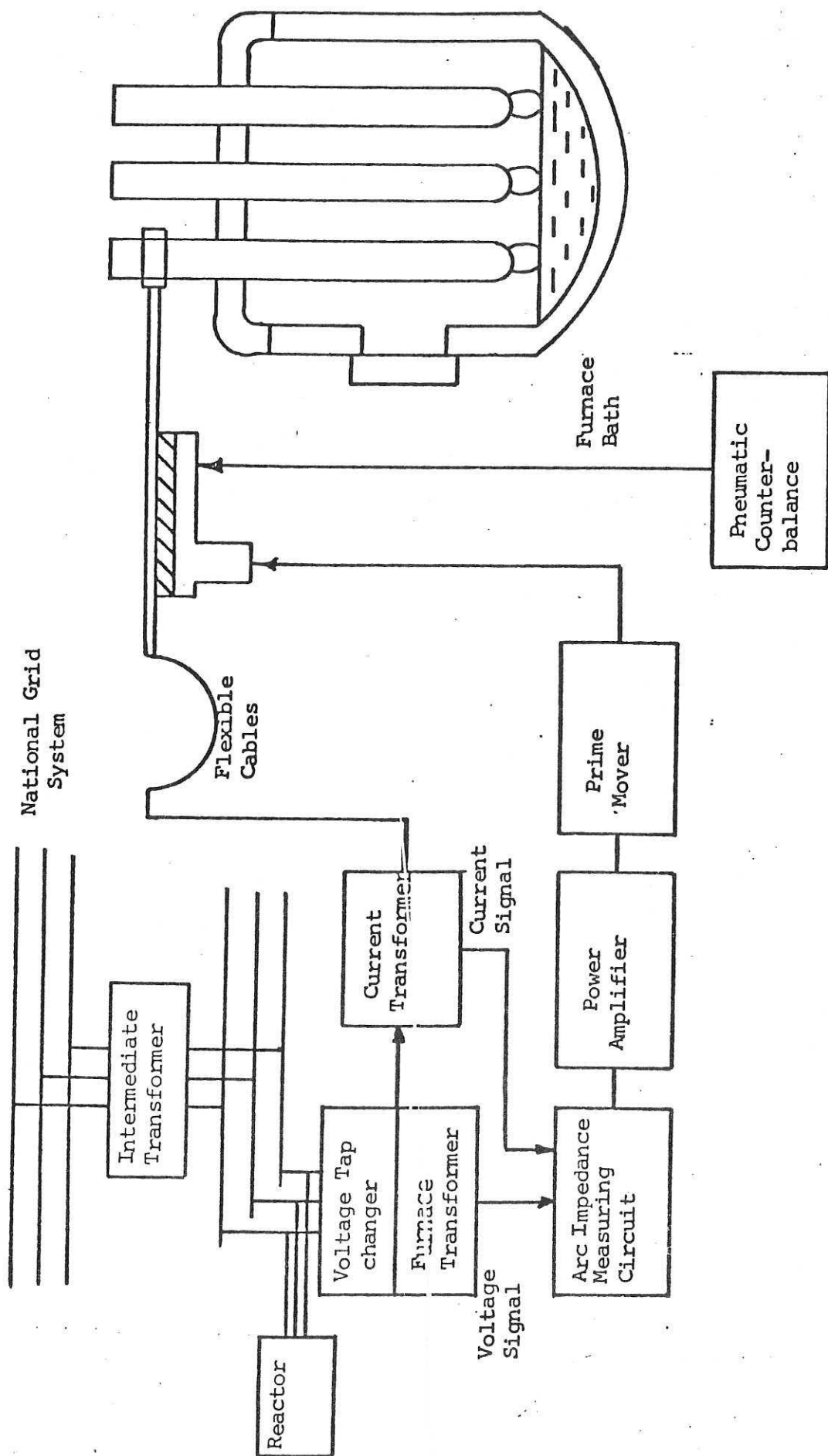


FIG 1 A SCHEMATIC DIAGRAM OF AN ARC IMPEDANCE CONTROLLED FURNACE

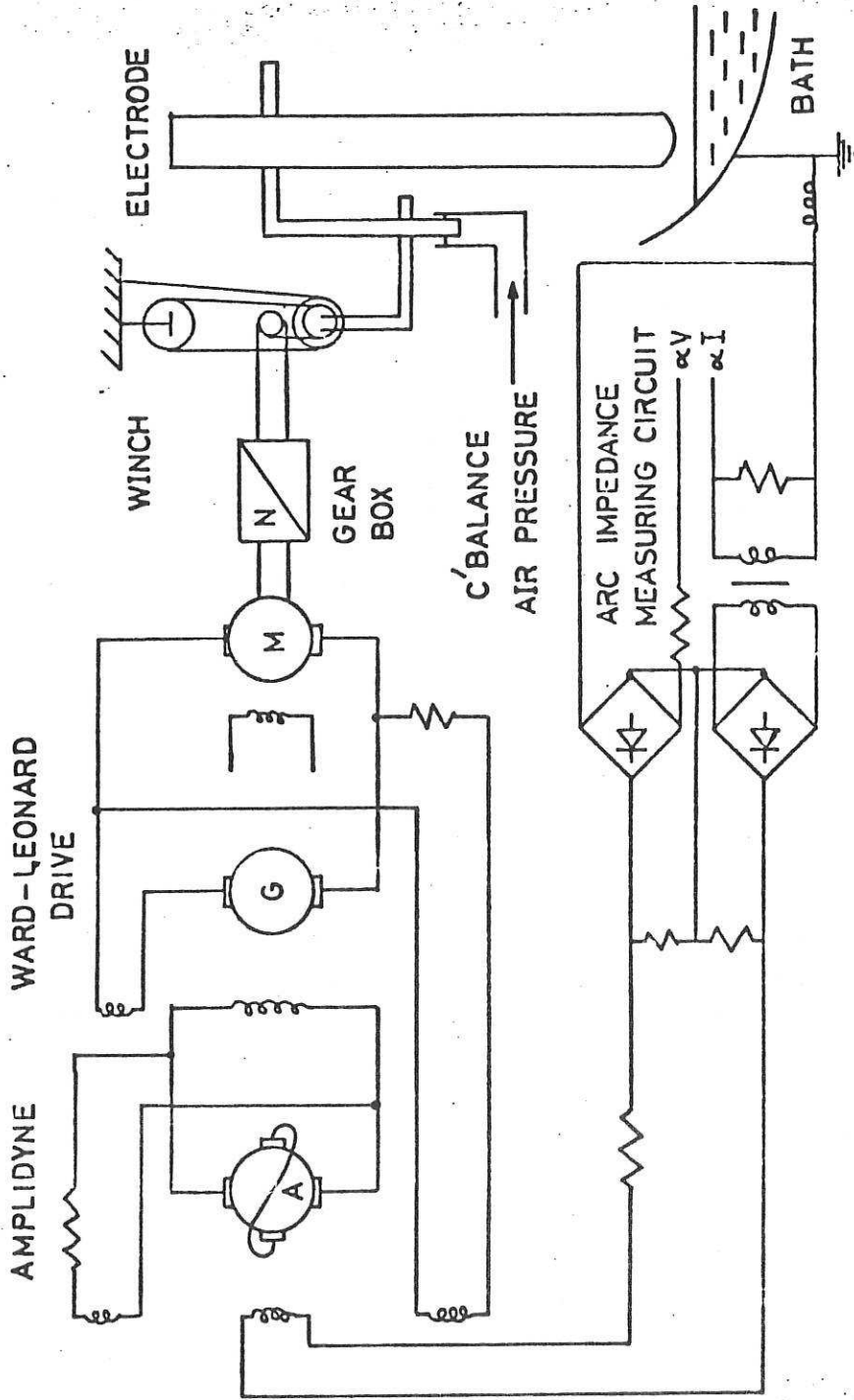


FIG. 2 WARD-LEONARD DRIVE ELECTRODE POSITION CONTROLLER.

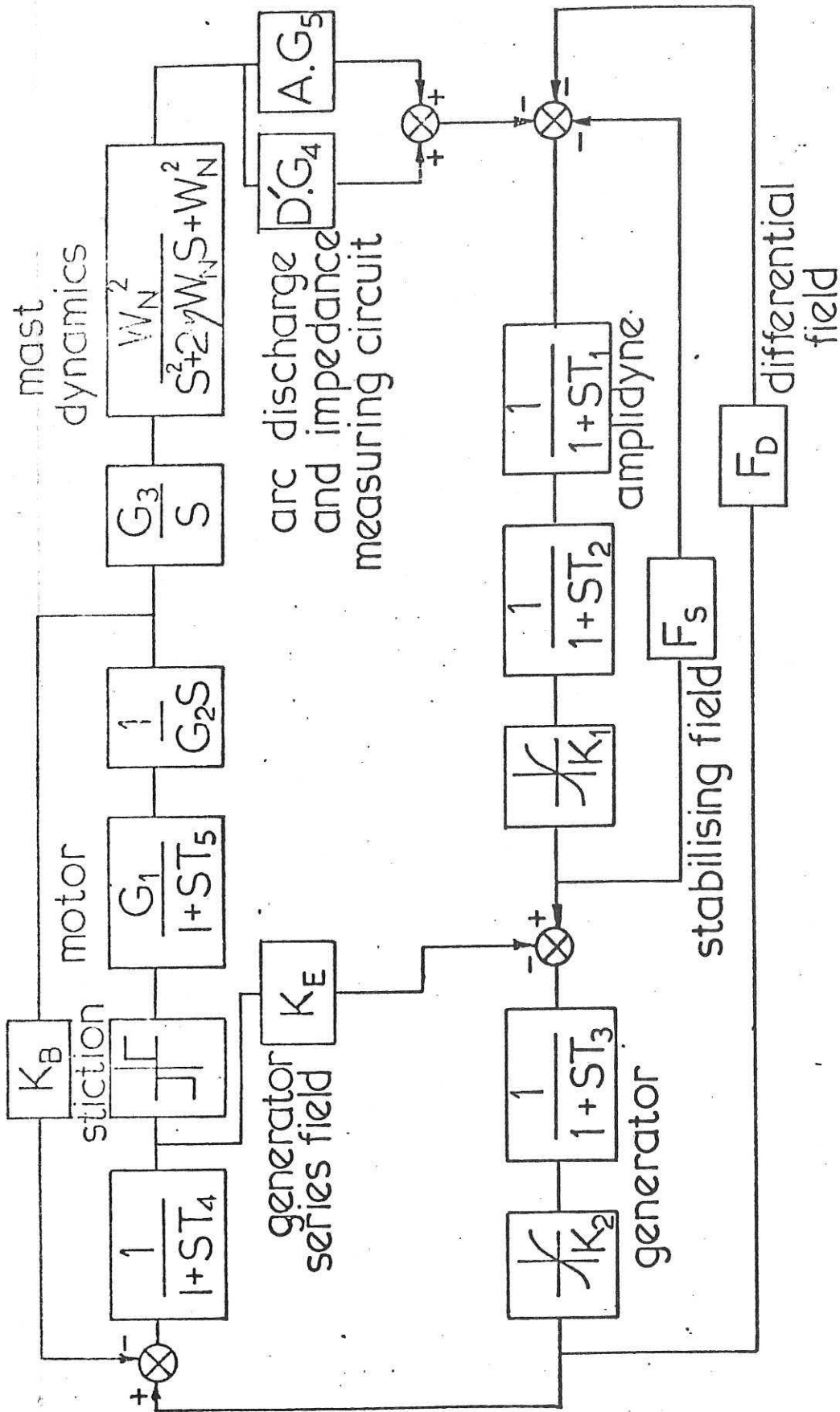


FIG 3 SINGLE PHASE TRANSFER FUNCTION MODEL

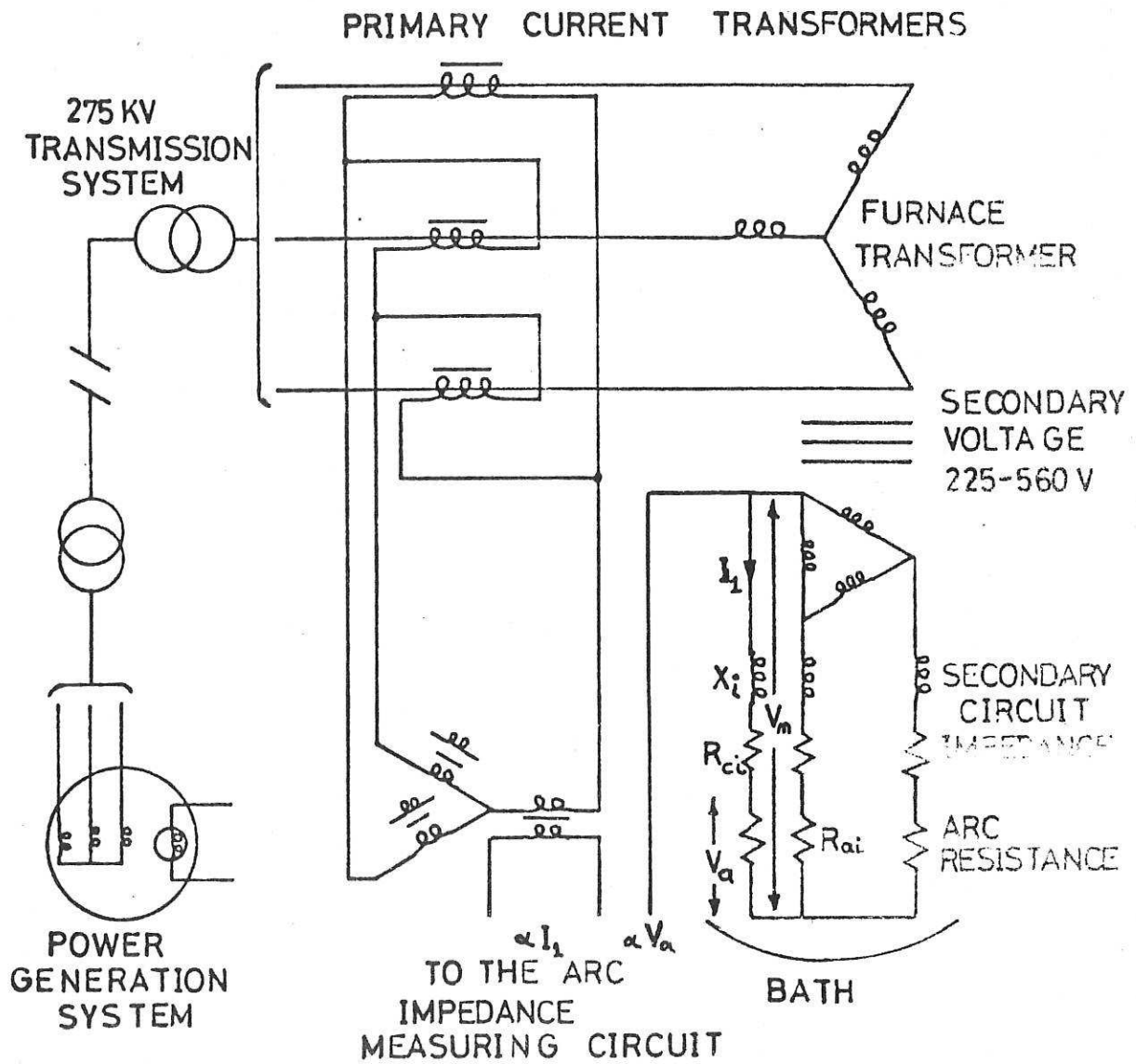


FIG 4 ELECTRICAL POWER SUPPLY SYSTEM

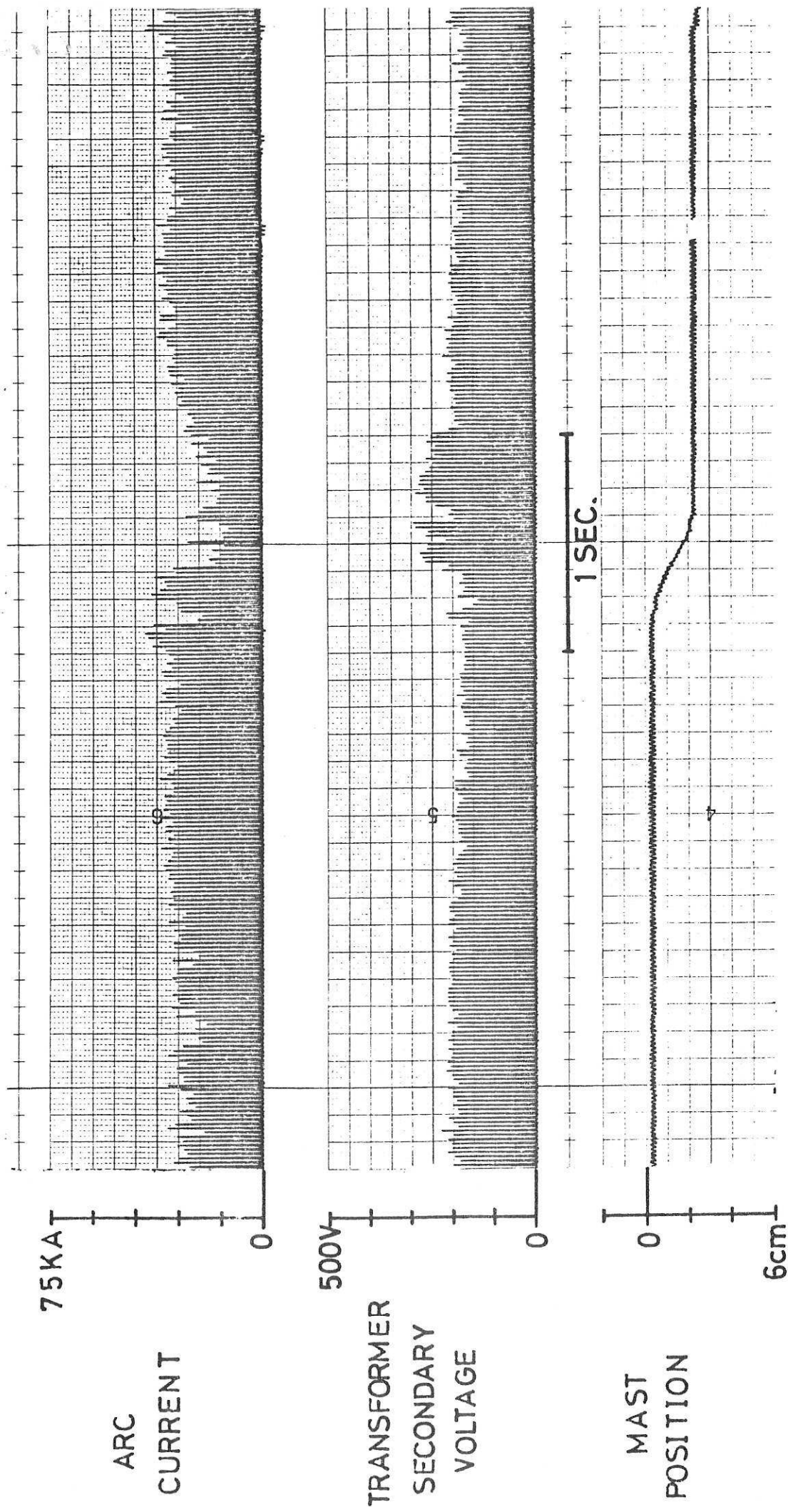


FIG. 5 A TYPICAL SEQUENCE OF NORMAL OPERATING DATA

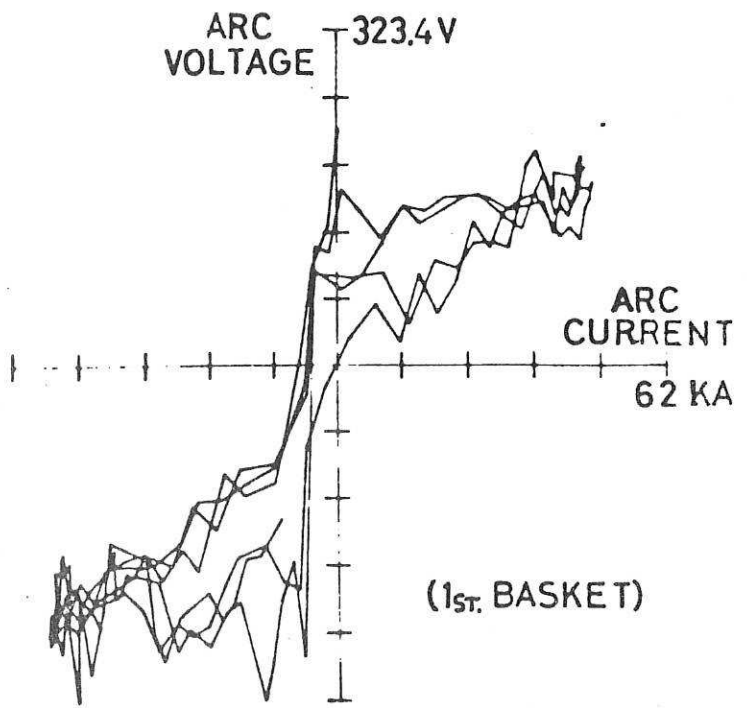
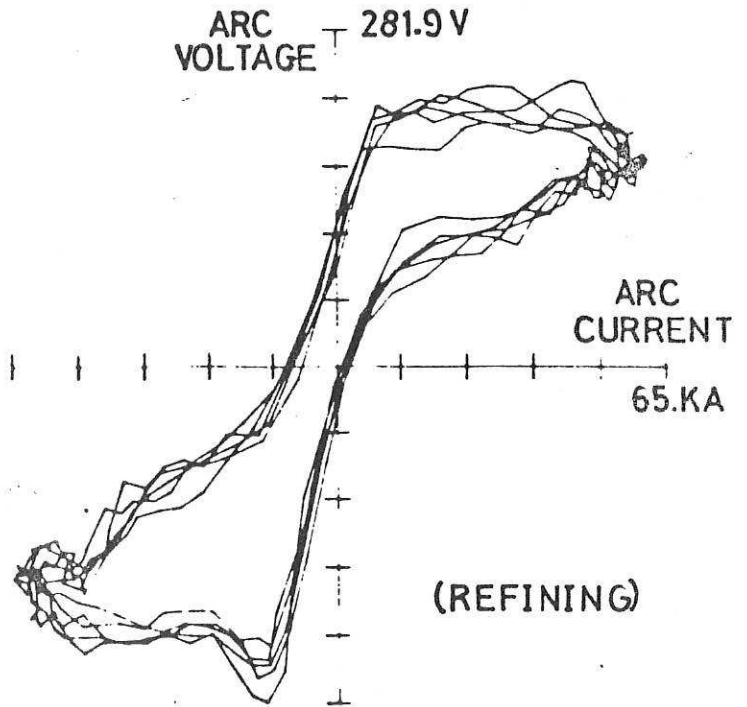


FIG. 6

DYNAMIC ARC CHARACTERISTICS

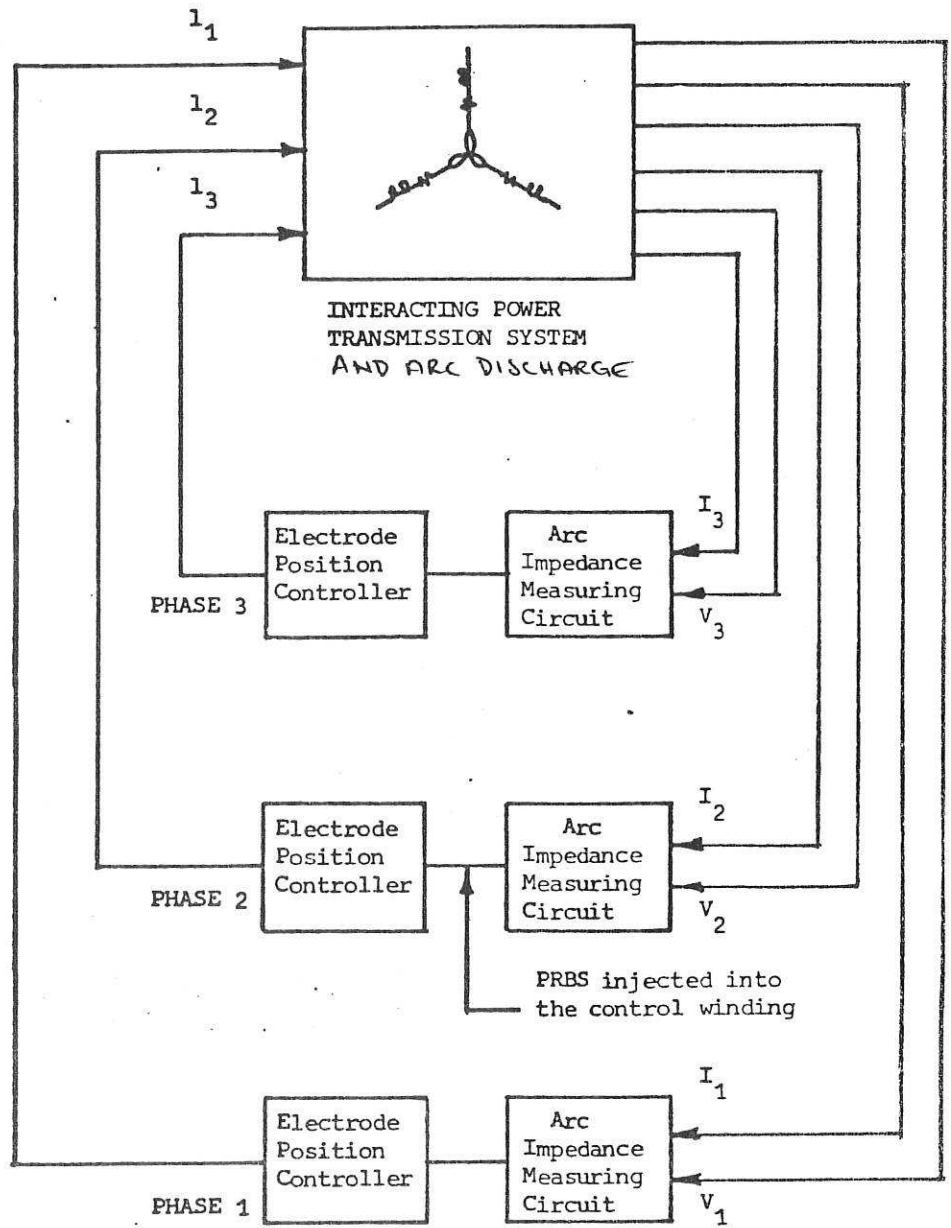


FIG 7 A SCHEMATIC DIAGRAM OF THE ARC FURNACE CONTROL SYSTEM

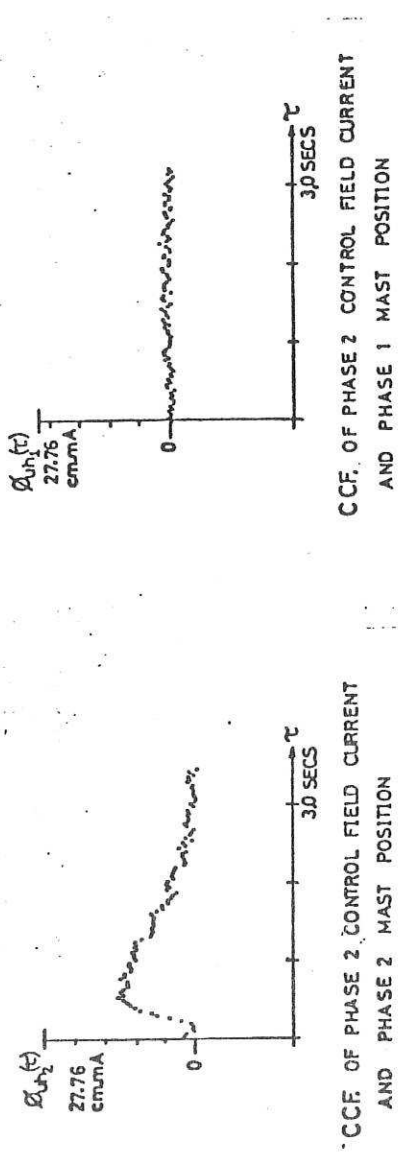


Fig 8 CROSSCORRELATION COMPARISON

ELECTRODE POSITION
CONTROLLER

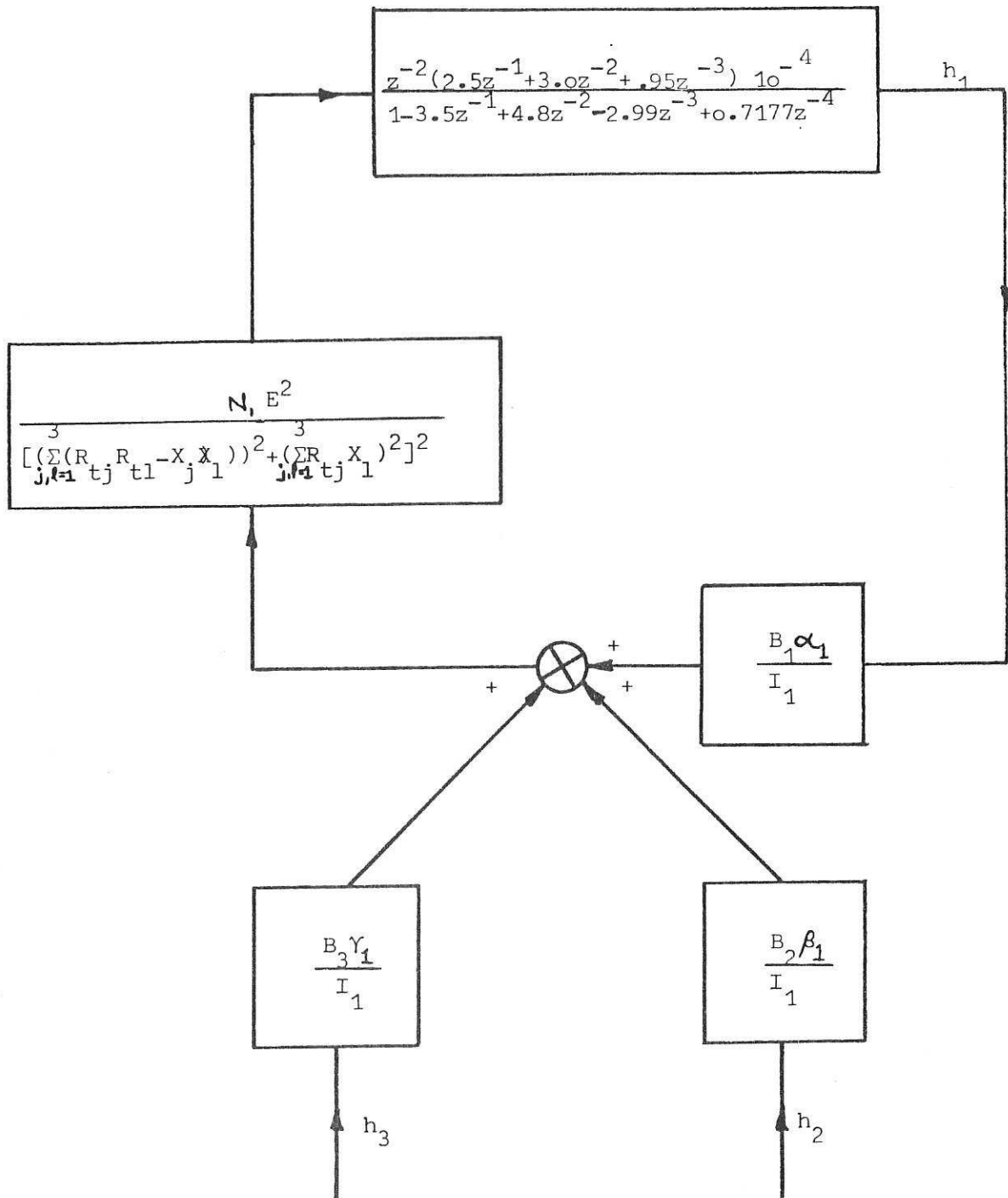


FIG 9 A SCHEMATIC DIAGRAM OF THE CURRENT CONTROLLED MODEL